Accepted Manuscript

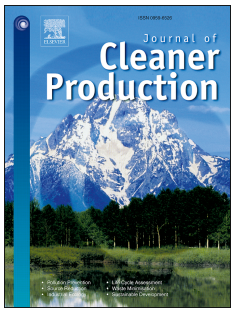

Chitosan-macroalgae biocomposites as potential adsorbents of water-soluble hydrocarbons: Organic matter and ionic strength effects

Carlos E. Flores-Chaparro, Mayra C. Rodriguez-Hernandez, Luis F. Chazaro Ruiz, Ma. C. Alfaro-De la Torre, Miguel A. Huerta-Diaz, Jose R. Rangel-Mendez

PII: S0959-6526(18)31850-X

DOI: 10.1016/j.jclepro.2018.06.200

Reference: JCLP 13346

To appear in: *Journal of Cleaner Production*

Received Date: 3 January 2018

Revised Date: 23 May 2018

Accepted Date: 18 June 2018

Please cite this article as: Flores-Chaparro CE, Rodriguez-Hernandez MC, Chazaro Ruiz LF, Alfaro-De la Torre MC, Huerta-Diaz MA, Rangel-Mendez JR, Chitosan-macroalgae biocomposites as potential adsorbents of water-soluble hydrocarbons: Organic matter and ionic strength effects, *Journal of Cleaner Production* (2018), doi: 10.1016/j.jclepro.2018.06.200.

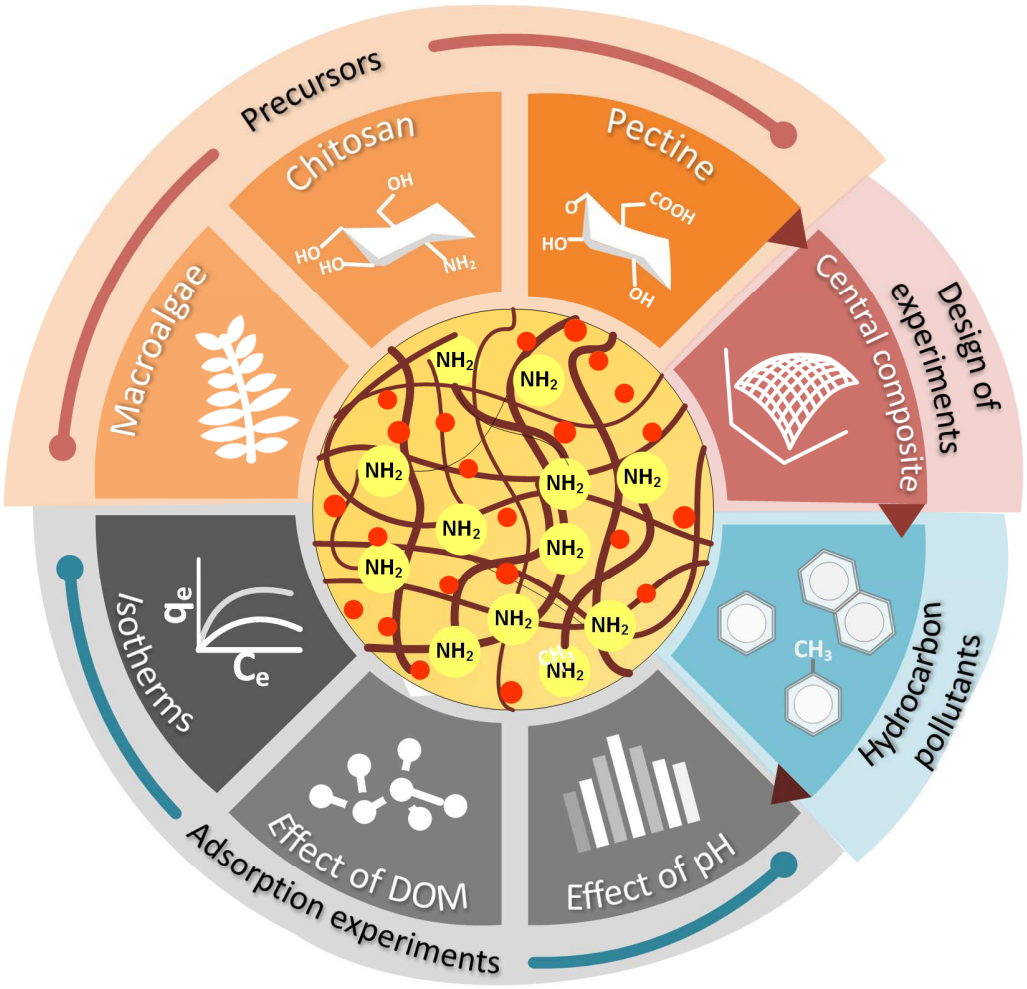

Macroalgae-based biocomposites

Chitosan-macroalgae biocomposites as potential adsorbents of water-soluble hydrocarbons: Organic matter and ionic strength effects

Carlos E. Flores-Chaparro [a,1], Mayra C. Rodriguez-Hernandez [a,1], Luis F. Chazaro Ruiz [a], Ma. C. Alfaro-De la Torre [b], Miguel A. Huerta-Diaz [c], Jose R. Rangel-Mendez [a]*

[a] IPICYT/División de Ciencias Ambientales, Camino a la Presa San José 2055, Col. Lomas 4a sección, C.P. 78216, San Luis Potosí, SLP, México. carlos.flores@ipicyt.edu.mx, cecilia.rodriguez@ipicyt.edu.mx, luis.chazaro@ipicyt.edu.mx, rene@ipicyt.edu.mx

[b] Universidad Autónoma de San Luis Potosí, Álvaro Obregón 64, Centro Histórico, C.P. 78000 San Luis Potosí, SLP , México. alfaroca@uaslp.mx

[c] Universidad Autónoma de Baja California, Campus Ensenada, Km. 103, Carretera Tijuana-Ensenada, Ensenada, Baja California, México. huertam@uabc.edu.mx

[1]Carlos E. Flores-Chaparro and Mayra C. Rodriguez-Hernandez equally contributed as first authors.

* Corresponding author. E-mail: rene@ipicyt.edu.mx. Phone: 52 (444) 834-20-00.
Fax: 52 (444) 834-20-10. IPICYT/División de Ciencias Ambientales, Camino a la Presa San José 2055, Col. Lomas 4a sección, C.P. 78216, San Luis Potosí, SLP, México.

ABSTRACT

Nowadays the recovery of low-molecular soluble aromatic hydrocarbons (HCs) released into natural bodies of water continues to be a challenging task. These contaminants bring sever consequences to the environment and to the human health. Biosorption on macroalgae (Ma) biomass seem to be a potential alternative to due to low costs and high availability, but the low strength and density are important drawbacks to handle, start up and operate continuous biosorption units. In this study, chitosan (Ch) and pectin (Pe) were employed as precursors to synthesize a new Ma−Ch−Pe composite with regard to enhance the stability and applicability of macroalgae biomass towards the removal of soluble HCs pollutants. The biocomposite synthesis was based on a factorial design and a posterior response surface methodology. The optimized biocomposite (75.4%, 19.8 and 4.8% for macroalgae biomass, chitosan and pectin, respectively), was characterized and evaluated under different ionic strengths, pH values and organic load to determine their potential as biosorbents and to elucidate the adsorption mechanisms involved. Removal capacities were 58.68, 16.64 and 6.13 mg g^{-1} for benzene, toluene and naphthalene, respectively. The adsorption capacity was slightly influenced by the pH (3-9), and diminished with ionic strength values up to $I > 0.6$ M. The presence of dissolved organic matter (DOM) enhanced the removal of HCs by providing hydrophobic sites to the biosorbents. Moreover, the biosorption data was well-described by Sips adsorption isotherm, and the pseudo-second order equation represented the best fitting model for the biosorption kinetics. The biosorption mechanisms included hydrophobic effect by the algae fraction and London forces between the HC and the diverse of functional groups present offered by the precursors.

Keywords: Chitosan composites; Biosorption; Macroalgae; Aromatic hydrocarbons; Oil spill

1. Introduction

Crude oil is one of the three main fossil fuels, along with coal and natural gas (Heede and Oreskes, 2016). When operational or accidental oil spills occur on bodies of water, even after applying clean-up technologies, water-soluble aromatic compounds from oil may persist and continue to produce negative effects on the ecosystem and human health (Liu and Kujawinski, 2015). Around 1 to 3% (sometimes up to 15%) of crude oil can pass into a dissolved state (Njobuenwu et al., 2005). Data from oil production have shown that the main aromatic compounds (> 96 %) in produced water are BTEX (benzene, toluene, ethylbenzene and xylene), followed by 2- and 3- ring polyaromatic hydrocarbons (PAHs) as naphthalene (3%), and at the end larger PAHs (<0.2 %) (Pampanin and Sydnes, 2013). Different methodologies have been suggested for soluble hydrocarbon removal and involve filtration, aeration, biodegradation and photocatalysis (Chen et al., 2010; US EPA, 2013; Wang et al., 2014; Ziolli and Jardim, 2002). These techniques have different degree of success, but sensible disadvantages including high-energy requirements, long periods of treatment, and expensive equipment. Sorption including different adsorbent media such as carbonaceous materials, natural products and wastes have proven to be an efficient, rapid and feasible alternative for soluble hydrocarbons removal in water (Caetano et al., 2017; Lamichhane et al., 2016; Rathod et al., 2014). A remarkable importance is noted for biosorption over the last few years because it was reported that this technology could be from 20 to 36% less expensive in comparison with conventional systems respectively (Ata et al., 2012; Vankar et al., 2013). Macroalgae (Ma) biosorption processes constitute a cost effective and environmental friendly alternative for the removal of petroleum-based soluble compounds (Flores-Chaparro et al., 2017; Hubbe et al., 2014). Furthermore, seaweed can be farmed in water avoiding any competition with food production (Angelova et al., 2016; Zhao et al., 2011). *M. pyrifera* is a broadly distributed macroalgae (Pacific and Southern oceans), and is the most largest algae which size ranges from 70-80 m with an annual growth rate of 50 m in suitable conditions (Zhao et al., 2011). Regardless of these promising outcomes, the physical

characteristics (small particle size, low strength and density) of such biomaterials are not viable for a continuous process operation and make biomass difficult to manage (Hameed, 2006). Therefore, the biomass immobilization techniques is one crucial issue to improve the practical application of macroalgae biomass on biosorption processes. The use of flocculant agents as an active immobilization technique has received special attention, in particular polysaccharides as chitin and its derivate chitosan, a highly available food processing by–product (Davila-Rodriguez et al., 2009). Chitosan is a linear polymer with a predominant amount of positive charged amino groups and a well-known affinity toward pollutants like metal ions and colorants. On the contrary, pectin (Pe) is a polyanionic compound composed predominantly by galacturonic acid units linked through α-(1-4) chain (Crini and Badot, 2008; Wan Ngah et al., 2011). Pectin molecule is extensively used in the food industry for its well-known thickening, stabilization and gelling properties (Motlagh et al., 2000), and also known by its positive health-related role with numerous pharmaceutical uses (Sriamornsak, 2011). The biopolymer-biopolymer interactions between the two oppositely charged polymers (chitosan and pectin) could increase the compatibility and stability of the biosorbents. This mechanism creates new structures that are called polyelectrolyte complexes. Though there are numerous publications on the formation of composites with chitosan for metals and nutrients biosorption purposes (Eroglu et al., 2015), it is still of interest to further integrate Ma−Ch−Pe composite via precipitation method to enhance their capabilities for practical applications on water–soluble hydrocarbons removal.

The main objective of this research was to determine by a factorial design, and by a response surface methodology, the proportion of *M. pyrifera*, chitosan and pectin that confer to the synthesized composites a greater ability to remove aromatic hydrocarbons. Later, the capacity of these composites to remove benzene, toluene and naphthalene under different scenarios of ionic strength, pH and dissolved organic matter in natural water was determined. A complete

physicochemical characterization of the biosorbent was performed to establish the adsorption mechanisms.

2. Experimental

2.1. Materials and chemicals

Chitosan (Ch) (with a molecular weight of 50,000 - 190,000 Da and a ≥ 75 % degree of deacetylation) and pectin (Pe) (galacturonic acid ≥ 74 %) were purchased from Sigma−Aldrich Co. Ltd. Other reagents, namely, acetic acid (HAc), NaOH and NaCl were obtained from J.T. Baker Co. Ltd. The macroalgae sample *Macrocystis pyrifera* (Ma), was collected in La Paz, Baja California Sur, Mexico and Ensenada, Baja California, Mexico. Dried biomass was rinsed with plenty of deionized water (<11 $\mu S \cdot cm^{-1}$) at 50 °C. Finally, the sample was sieved to a particle size of < 250 μm with a Mini-Cutting Mill (Thomas Wiley) before used in sorption experiments and characterization. The model organic pollutants included in this work were benzene, toluene and naphthalene (Sigma–Aldrich, 99% purity).

2.2. Preparation of Ma−Ch−Pe biocomposites

The Ma−Ch−Pe biocomposites were prepared by dissolving a definite amount of pectin (Pe) powder (up to 2 g) in deionized water. At the same time, 3 − 5 g of chitosan were suspended in the pectin solution. Then, 50 mL of HAc 5% (v/v) were added to the mixture, and stirred continuously for 30 min. The synthesis was followed by the addition of a specific amount of the macroalgae biomass (Ma) (Supplementary materials: Table S1 and S2), and the final composite was stirred for another 12 h. The homogeneous (Ma−Ch−Pe) solution was fully poured through a drop system (Fig. 1a) into a 25% NaOH solution for hydrogelation, according to a previous methodology (Pérez-Escobedo et al., 2016). The obtained hydrogels were washed with distilled water to neutral pH and dried at room temperature for 48 h. The average particle size could be controlled from 3 – 6 mm by changing the tip of the syringe.

2.3. Optimization of biosorbent composition for hydrocarbon removal

2.3.1. Factorial design

A screening experiment involving a three factor two-level full factorial design (2^3 runs) was employed. Preliminary experiments were conducted to select the suitable high and low levels (Table S1). Moreover, Table S2 shows the design matrix for the total 10 experiments, and the q_e measured in each run, with the low and high levels as specified in Table S2. The design included two center points in order to have an estimate for the experimental error (Hashemi et al., 2005). Benzene was selected as aromatic hydrocarbon model, its removal by the composite was the response variable. All determinations were replicated at least twice. The results were examined with Design Expert software v.6.0 in order to determine the main interactions and effects.

2.3.2. Response surface design (RSD)

Response surface methodology (RSM) is a mathematical and statistical approach useful for working with specified ranges of the input variables to find the factor settings capable to improve the performance of a process, for example, to maximize the capacity of adsorption of an adsorbent (Ravikumar et al., 2005). RSM is often employed after a thorough screening using full or fractional factorial experiments (Myers et al., 2016). Therefore, in order to achieve the highest amount of benzene adsorbed by a Ma−Ch−Pe biocomposite, a non-replicate face-centered cube central composite design was used. Initial amounts of Ch (20 - 40%) and Ma (60 − 80%) were selected as independent input variables. Regardless the non-significant effect of pectin observed in the factorial design (section 3.1), 5 wt % of this polymer was added to the Ma/Ch mixture to increase the solution viscosity and mechanical strength (Tsai et al., 2014). Finally, the hydrogelation procedure was performed as described above.

Five central points were established to provide a reasonably stable variance of the predicted response (Antony, 2014). The range, levels and responses of the researched variables are presented

in Table S3. Treatments were performed randomly, and the results were analyzed using the statistical program Design Expert® v.6.0. The significance of the models was tested by variance analysis (test F), R^2 coefficient and significance of the independent variables were also calculated ($\alpha = 0.05$).

2.4. Biocomposite properties testing

The selected Ma−Ch−Pe composite was evaluated by several physicochemical analysis as follows: surface area ($m^2\ g^{-1}$) and pore size distribution of the samples were calculated by BET isotherm and DFT (Density Functional Theory), respectively, with a Micromeritics ASAP 2020 apparatus at 77 K (Brunauer et al., 1938; Lastoskie et al., 1993). Potentiometric titrations were performed in an automatic titration system (Mettler Toledo T70) for proton binding curves and point of zero charge (pH_{PZC}) determinations. A mass of 0.1 g was placed in 50 mL of a 0.1 NaCl solution. The proton binding curves were generated through the transformation of the experimental titration data (50-70 points) by using the SAIEUS program.(Bandosz et al., 1993; Jagiello, 1994). Interactions between biocomposite precursors were studied by using a Thermo Nicolet 6700 FT-IR in transmittance mode within the range of 600-4000 cm^{-1}, with a 4 cm^{-1} resolution and 128 scans.

The X-ray diffraction (XRD) patterns of the biocomposite were obtained with a step time of 10 s and 2θ of 0.01° with a XRD D8 Advanced-Bruker Axs (Cu Kα radiation λ = 1.546 Å). Powder samples were employed in the analysis.

The degree of swelling (S_w) was determined in triplicate runs by weighing a precise mass of 0.5 g of dry biocomposites and placed in a baker at 25 °C with 25 mL of distilled water. The swollen materials were removed from water and weighted (W_t) after 24 h. S_w value was computed by the following equation: $S_w = ((W_t - W_o) / W_o)*100)$. Where, W_o is the mass weighted of the dry biocomposite ($t = 0$) and W_t is the mass weight of the swollen material at time t.

Chemical stability was determined by contacting the solids in acidic water, which is based in a previous methodology (Davila-Rodriguez et al., 2009). Briefly, a specific mass of biocomposite was placed in acidified water (pH = 5) at 25 °C. The mixture was shaken at 120 rpm until the pH of the solution has no change. The solids were separated by filtration and dried at 70 °C for 48 h. The chemical stability was the percentage of mass loss at initial and final stage.

2.5. Equilibrium experiments

For experimental design essays, benzene was selected as the model pollutant, but in the case of the selected biocomposite, toluene and naphthalene were also tested. The removal capacity of the optimized Ma−Ch−Pe biocomposite was determined under deionized water including the maximum solubility of each compound (Xie et al., 1997). In all the cases, evaluations were conducted by adding 0.1 g of each sorbent to a series of 35 mL amber glass flasks that contain a specific amount of benzene, toluene or naphthalene, specified in Table S4 (Supplementary materials). The experiments were carried out at 90 - 100 rev min^{-1} and 25 °C. The concentrations of benzene, toluene and naphthalene in solutions were determined using a UV-Vis (Thermo Aquamate) spectrometer at a wavelength of 254.5, 261 and 284 nm, respectively. At least two blanks with the same amount of biocomposite (no HC added) were run simultaneously as controls along the sorption samples to correct the final HC concentration and ultraviolet adsorption for desorbed organic matter. The adsorption capacity q_e (mg g^{-1}) of the aromatic compounds was computed by the following Eq. (1):

$$q_e = \frac{V}{m}(C_0 - C_e) \qquad (1)$$

where C_0 and C_e are the initial and equilibrium concentrations (mg L^{-1}), V is the volume of the solution (L), and m the mass of the adsorbent (g). The equilibrium data for adsorption was evaluated with the Langmuir, Freundlich, and Sips isotherm models described elsewhere (Flores-Chaparro et al., 2016). Quasi-Newton algorithms were employed to compute equation parameters using the

STATISTICA software V.10. Model selection was based on the statistical values of the correlation coefficient (R^2) and the sum of the sum of the squares error (SSE), according to the following:

$$\sum_{i=1}^{n}\left(q_{e,calc} - q_{e,meas}\right)_i^2 \qquad (2)$$

Where $q_{e,calc}$ and $q_{e,meas}$ are the estimated and actual sorption capacities values at equilibrium (mg g^{-1}).

2.5.1. Effect of the pH and ionic strength

The effect of ionic strength was studied under different ionic strength solutions (I = 0.3, 0.45, 0.6 and 0.75 M), as well as with a synthetic seawater solution Instant Ocean® ($I \simeq 0.76$ M). The salting coefficients κ_s of the hydrocarbons were calculated to determine the organic dissolution rates at different NaCl solutions (Table S4). Calculations were performed according to the Setchenow equation $log(S_o/S) = \kappa_s C$, where S_0 is related to the solubility of benzene, toluene and naphthalene in water (Benbouzid et al., 2012). Additionally, desorption tests were performed for saline solutions as follows: The 0.1 g pre–adsorbed Ma−Ch−Pe biocomposites were filtered by decantation, rinsed with deionized water to remove contaminant excess and subsequently immersed into 35 mL of water at the same I as the previous biosorption runs (100 rev·min^{-1} and 12 h). The organic leached was determined by an UV−Vis spectrophotometer as already mentioned. The amount of desorbed HCs was determined by the difference between the HCs concentration in the initial solution and that remained in the agitated solution.

The effect of the initial pH in the biosorption of aromatic hydrocarbons was also investigated in deionized water at pH values from 3.0 to 9.0. under the aforementioned conditions. The pH of the solutions was adjusted with HCl and NaOH solutions.

2.6. Biosorption kinetics

To determine the effect of contact time, a 0.1 g of the selected biocomposite were placed into amber bottles with deionized water at the initial concentration specified in Table S4 for benzene, toluene and naphthalene, respectively. The kinetics were obtained from batch experiments (time scale: 0 to 50 h), containing 35 mL of HC solution stirring at 90 - 100 rev min^{-1} and 25°C. At given time intervals, sample were collected for analysis and the HC remaining concentration was determined by UV-Vis spectrophotometer as mentioned above. An approach to describe the biosorption rate was determined by the pseudo first-order, pseudo second-order and Weber Morris rate equations as previously reported (Qiu et al., 2009; Tsibranska and Hristova, 2011).

2.6.1. Effect of dissolved organic matter (DOM)

To evaluate effects of DOM on the rate removal of benzene, toluene and naphthalene, experiments were carried out by using natural water from a reservoir containing 19.3 $mg \cdot L^{-1}$ of DOM (Fig. 5a,b). The natural water collected from a reservoir located in San Luis Potosi, Mexico, was filtered through Millipore 0.22 µM nylon filters and was chemically characterized; total organic carbon was measured using a Total Organic Carbon Analyzer (TOC-VCSN Shimadzu), metals concentration was determined by Inductively Coupled Plasma-Optical Emission Spectrometry (ICP-OES, Varian 730-ES).

In order to verify the aromaticity and humic acids content of the sample, the Chromophoric DOM (CDOM) was measured through UV-Vis spectrophotometric analyses at two specific wavelengths (250 and 350 nm) for the computation of E_2: E_3 ratio and the specific ultra-violet absorbance ($SUVA_{254}$) described elsewhere (Santos et al., 2016). Absorption spectra of DOM solution is shown in Fig. S1. Finally, anions concentration was analyzed by capillary electrophoresis (Agilent 1600). The summary of the characterization is showed in Table S5. Sorption kinetics studies using natural water were carried out and the data were analyzed under conditions indicated in section 2.6.

3. Results and discussion

3.1. Design of Experiments

A factorial experiment design in conjunction with an analysis of variance was the first approach in optimizing the conditions for benzene removal capacity onto a diverse of Ma−Ch−Pe compositions. The range studied was between 3 and 5 g for chitosan, up to 2 g for pectin, and between 2.7 and 5.4 g for macroalgae biomass (Table S1). The experimental tests are given in Table S2. Based in the former information, an analysis of variance (ANOVA) and P_{value} significant levels were calculated to check the significance of the effect on benzene biosorption. The statistical parameter P_{value} (more than 0.05) suggests that the model was not significant if we include the overall (Ma−Ch−Pe) interactions. However, in the case of Ma, Ch and Ma–Ch interaction, significant model terms with more than 95% confidence level were estimated (Table S6). Based on this, the content of pectin (Pe) was negligible. This finding indicates that the amount of chitosan and macroalgae biomass parameters had the most significant effect in the benzene biosorption capacity. Because of this, model reduction was suitable leaving only the significant model terms (Ma-Ch interaction).

After the main parameters were identified, subsequent experiments were performed to analyze the nature of interactions among them by a response surface methodology (RSM). The Ma/Ch ratio is critical to the performance of the biocomposite. For extensive application, it is desirable to use more *Macrocystis pyrifera* in production of a biosorbent as it plays a key role in biosorption and represent the more accessible precursor of the biocomposite (Yang et al., 2011). Hence, an upper Ma/Ch ratio was used for the surface response design experiment. Pectin was established to a minimal value (5 % w/w) since this did not have a significant influence on benzene removal, but enhanced the mechanical properties of the final material as also reported by (Eroglu et al., 2015 and Wan Ngah et al. 2011).

The design matrix and the corresponding experimental data of the central composite design (CCD) are given in Table S3 after tests. The CCD results were fitted to an elliptical second–order polynomial equation: Benzene removal (mg g^{-1}) = 49.05 + 3.31A + 0.54B − 7.55A^2 − 7.35B^2 − 4.79AB. The fit of the model was evaluated by the correlation coefficient, R^2, which was 0.989, indicating that 98.9% of the variability in the response could be explained by the model (Table S7). The statistical significance of the second–order model equation was evaluated by an F–test, which reveals that this regression was statistically significant ($P < 0.0001$) at the 99 % confidence level. Table S7 also shows that Chitosan (A), Macroalgae (B) and the Chitosan-Macroalgae (Ch–Ma) interaction, had a highly significant effect ($P < 0.0001$) on benzene removal.

The contour plot described by the benzene removal is represented in Fig. 1b, which shows that the maximum benzene removal capacity was approximately 50 mg· g^{-1}, which corresponds to the central point within the highest contour levels (Ravikumar et al., 2005). The optimal concentration for the two precursors obtained from the maximum point of the model was 20.8 % (w/w) for Ch (A) and 79.2 % (w/w) for Ma (B). The model predicts a maximum response of 49.42 mg· g^{-1} at this point. Therefore, the final biocomposite composition was 75.4%, 19.8%, and 4.8% for macroalgae biomass, chitosan and pectin, respectively.

3.2. Characterization experiments

3.2.1. FT-IR and XRD analyses

The FT-IR spectrums between 4000 cm^{-1} and 600 cm^{-1} for Ma, Pe, Ch, Ch-Pe and the optimized Ma−Ch−Pe biosorbents (Table 1; Fig. S3), were compared to elucidate the chemical structure and reaction mechanisms occurring on the biocomposites. The FT-IR spectra of Ch is close to a previous work reported in the literature (Jiang et al., 2016). The major peaks of Ch were registered at 3352 cm^{-1}, 1654 cm^{-1}, 1590 cm^{-1}, 1424 cm^{-1}, and 1068 cm^{-1}, which corresponds to the N-H stretching vibration, C=O stretching vibration of –NHCO- (acetylated section), N-H deformation of

primary amides (formed during deacetylation), -CH bending and C-O stretches, respectively. FT-IR spectra of pectin show bands at 1730 and 1600 cm^{-1} assigned to methyl esterified and vibrations of the O=C-O structure, respectively (Marudova et al., 2004). The IR spectra of macroalgae biomass indicated a broad band between 3800-3000 cm^{-1} which corresponds to hydroxyl (-OH) and amine (-NH_2) groups, which could be associated to polysaccharides and amino acids, respectively (Zhang et al., 2013). Moreover, the band intensity at 2848 cm^{-1} represents the aliphatic chain of lipids, whereas the peak at 1638 cm^{-1} could be related to the presence of carboxylate groups (-$RCOO^-$) associated to alginate and primary amides of amino acids. Finally, the band at 1155 cm^{-1} was attributed to sulfates polysaccharides and amino acids (Flores-Chaparro et al., 2017)

In the Ma−Ch−Pe spectrum, the peaks at 2940 cm^{-1} and 1366 cm^{-1} were assigned to C-H from Ma sulfated fucans, and COO^- groups from Ch-Pe. These peaks were downshifted compared to Ch−Pe due to a possible hydrogen bonding between Ma and Ch functional groups. The FT-IR spectrum of Ma−Ch−Pe material indicated that the intensity of the peaks at about 2021 cm^{-1}, 1650 cm^{-1}, 1593 cm^{-1}, 1309 cm^{-1} and 1064 cm^{-1} changed and even some of them disappeared compared to the peaks of Ch-Pe. These results may suggest that in the Ma−Ch−Pe samples, different interactions could occur between functional groups such as N-H, C=C, C-O-C, S-O and C=N.

The XRD patterns of the Ma-Ch-Pe biocomposite are reported in Fig. S2#. The XRD profile of Ma-Ch-Pe composite presented two broad peaks at 2θ = 14.69 and 22.8°, which correspond to the presence of amorphous cellulose (Terinte et al., 2011). However, the reported peaks for chitosan are closer to cellulose values (11.3 and 23°), and both peaks would be overlapped (Yang et al., 2010).

Many processes are involved in the biocomposite synthesis reported herein. Chitosan solubilization (pH < 6.5) occurs by protonation of the $–NH_2$ group ($R{-}NH_2 + H^+ \leftrightarrow R{-}NH_3^+$) on the C-2 position of the D-glucosamine repeat unit, transforming the polysaccharide to a polyelectrolyte in acidic media (Rinaudo, 2006). Chitosan in solution is able to form electrostatic interactions with the negative unesterified uronic acid residues of pectin ($-COO^{-}\,^{+}NH_3$), allowing the creation of

junction zones to form a network (Kyzas and Bikiaris, 2015). Numerous interactions are involved in the gelation process such as electrostatic repulsion, "ionic crosslinking", hydrophobic effects (by $-CH_3$ group), and hydrogen bonding interactions (groups involved are −OH, −NH, and –C=) (Cho et al., 2005).

3.2.2. Potentiometric titrations

The surface charge of the biosorbents was determined through potentiometric titrations as a function of pH (Fig. 2). Acid dissociation constants were calculated from potentiometric data (Table S8). The titration curve of pristine chitosan shows that under low acidic conditions the surface registered positive values, but with an increase of pH, the surface charge changed to negative values. The two main basic sites detected from Ch were amine ($-NH_2$) (pK_a 8-11) and hydroxyl groups, confirmed by previous reports (Volesky, 2007). The point of zero charge was located at pH_{PZC}= 8.2. On the other hand, a marked presence of carboxyl groups (pK_a 3-5) and hydroxyl groups, lowered the surface charge of pectin to negative values, in accordance to previous reports (Balaria and Schiewer, 2008).

The neutralization of the surface charge by Ch-Pe, was probably due to the synthesis of the ion pair ($-COO^- -NH_3^+$) as mentioned above. Moreover, a decrease of the negative surface charge could be associated to the formation of hydrogen bonds between the −OH groups of Ch, and the oxygen atom (-O···HO) from the D-galacturonic acid unit of pectin (Pandey et al., 2013). Related to the macroalgae, the carboxyl groups of alginate were the more abundant in the cell wall, and the pH_{PZC} above 8 could be associated to amines (from proteins), sulfhydryl (pK_a 8-10) and hydroxyl groups (pK_a 9.5-13) from alginates, proteins, phospholipids, and polysaccharides, respectively (Schijf and Ebling, 2010). The major presence of weak acidic (i.e. carboxylic and lactonic) functional groups in the Ma−Ch−Pe biocomposites could be related to the presence of lactone and alkaloid groups from Ma polysaccharides, and the dimeric repeating unit of Ch. Moreover, the reported quantity of very weak functional groups (pKa > 7) suggested a structural re-arrangement of hydroxyl and amine

groups probably derived from hydrogen bond or London chemical interactions between Ch and Ma during the synthesis process.

3.3. Biosorption studies

The benzene, toluene, and naphthalene adsorption capacity of the selected biocomposite was determined in deionized water at the maximum solubility of each compound (Table S4). Fig. 3 shows the nonlinear fitting of the experimental data to Sips adsorption isotherm equation by STATISTICA software v.10. Table 2 presents the resulting maximum adsorption capacities (q_{max}) and isothermal parameters. According to the regression coefficient (R^2) and the sums of squares error (SSE), the biosorption process best fits the Sips isotherm. Sips adsorption isotherm equation can describe both Langmuir and Freundlich characteristics for heterogeneous surface systems like in the case of biosorbents. The exponential character of Freundlich equation can only accurately describe the lower concentration ranges by an exponential rise in the amount adsorbed with increasing concentration, while at high sorbate concentrations it shows an asymptotic behavior distinctive of the Langmuir isotherm (Jeppu and Clement, 2012).

A good fit of the data to the Sips adsorption isotherm ($R^2 > 0.98$) allowed to calculate the maximum removal values (assuming that adsorption occurs on a monolayer) of 58.68, 16.64 and 6.13 mg g^{-1} for benzene, toluene and naphthalene, respectively (Table 2). The exponent n value represents the underlying affinity distribution for heterogeneous systems, which can vary from 0 to 1 (Liu and Liu, 2008). The registered ($n > 1$) values for the three molecules under study means that the physical biosorption is more related to Langmuir adsorption behavior in comparison with Freundlich equation, which was also confirmed by the SSE value of Langmuir and Freundlich isotherm equations listed in Table 2. A dimensionless constant derived from Sips isotherm known as separation factor (R_L), was computed in order to predict the affinity between the sorbate and sorbent, indicating a favorable biosorption process. The textural properties of the biosorbent do not present steric limitations for the pollutants diffusion (Table S9). The low surface area of the

biosorbents do not entirely explain the affinity of non-polar hydrocarbon, for that reason the adsorption capacity is severely influenced by the biosorbent chemical composition, resulting from the precursors. Former studies established that many acid dyes molecules with one or more benzene aromatic rings are attached in a parallel manner to the amine groups of chitosan, then tend to form subsequent complexes and interactions (Crini and Badot, 2008; Navarro et al., 2009). Otherwise, hydroxyl groups could generate van der Waals interactions and Yoshida hydrogen bonding, particularly in the C–3 position, between chitosan chains and aromatic molecules (Shimizu et al., 1995). Pectin also possess additional − OH active sites in conjunction with carboxylic groups that contribute with dispersive interactions with the pollutants (Motlagh et al., 2000). The HCs biosorption mechanism in the brown macroalgae biomass involves the sum of the interactions occurring with the diversity of chemical components, including hydrophobic effect between lipids and lignocellulosic fractions (cellulose, hemicellulose and lignin) (Rubín et al., 2006), and to a lesser degree, nonspecific van der Waals interactions with carbohydrates (in special with alginates) and proteins (Tsuzuki, 2005). The loaded biosorbent with benzene and toluene was lyophilized and characterized by FT-IR in the range of 600 and 4000 cm^{-1}, and the results suggest that all functional groups are involved in the biosorption process, however the –OH and C-O chemical groups registered the main changes, suggesting the main role of cellulose and hemicellulose in the biosorption process (Fig S4).

In order to elucidate the contribution of the Ch-Pe fraction to the total removal capacity of the Ma−Ch−Pe biocomposite, additional biosorption essays were performed for the three HCs under study at the same conditions described in section 2.5. The biosorption was 7.35, 3.83, and 0.94 mg g^{-1}, for benzene, toluene and naphthalene, respectively, which represents the 15, 24 and 22 % of the total removal capacity of the aforementioned pollutants. Therefore, the macroalgae fraction contributes more to the removal of the hydrocarbons, compared to chitosan and pectin immobilizing

agents. These results agree with our previous ANOVA analysis where the P-value of pectin and chitosan factors were higher than 0.05 in the factorial and the response surface methodologies.

3.3.1. Effect of ionic strength

The effect of competing ions was investigated (Fig. 4a). A progressive decrease in the removal capacity was registered from an ionic strength value of 0.6 M. It is supposed that a high concentration of salts promotes a partial neutralization of the surface charge, followed by the reduction of the electrical double layer by the Na^+ cation. Moreover, the solvated Cl^- anions (radii of 0.202 nm) could improve interactions with the biosorbent surface promoting pore occlusions and avoiding many of the unspecific interactions related to a lower swelling degree (%) in relation to the SW in deionized water. Preliminary studies have shown similar results for different brown macroalgae biomass (Schiewer and Wong, 2000). Instant Ocean® is a special case of study because this solution also contains different ions ($I \approx 0.76$ M) and organic matter that may block pores, preventing the diffusion of the adsorbate to the active sites. In addition, hydrophilic interactions from the inorganic content of the artificial seawater solution may be enhanced with the increase of *I*, generating biosorption competition by water clusters (Arafat et al., 1999). It was observed a slightly increase in desorption capacity for all the pollutants (Fig. S5, Supplementary materials),because the high ionic concentration of ions in addition with a low surface area (0.9 and 0.2 $m^2\ g^{-1}$ for chitosan and macroalgae biomass respectively) overcome some of the dispersive adsorbed molecules (Chung et al., 2007). However, 88, 76 and 69% of benzene, toluene and naphthalene, respectively, remained adsorbed to the composites after 12 h exposure to deionized water.

3.3.2. Effect of pH

Fig. 4b shows that the pH of the system (5–9) has no significant effect on the removal ratio of the adsorbates. The biosorption capacity minimally changes and is maintained at approximately 50, 20 and 8 $mg \cdot g^{-1}$ for benzene, toluene and naphthalene, respectively. The reinforced Ma-Ch-Pe

biocomposite was tested by quantifying its mass loss after being placed in contact with water at slightly acidic pH (5) during 24 h. Mass loss between 1.2- 2.9 % from the chemical stability essays reflect that the polymeric matrix of Ch covered and strengthened the macroalgae biomass. This data is in accordance with the swelling degree (380) of the biocomposite, which is lower than the value of the raw macroalgae biomass of 570, reported previously (Flores-Chaparro et al., 2017).

The hydrolytic stability was tested to assess the effect of temperature in the biosorbent constitution (Fig. S6). Two samples were stored at 25 and 35 °C for 100 h at neutral pH. A thermal degradation was negligible between the two temperatures, with a mass loss percent around 15 % in both samples. The water stability of the biocomposites could be associated to hydrophobic polymers like cellulose and chitosan, but higher temperatures may increase inter-chain mobility and the hydrophilic character of the biosorbents.

During the synthesis process, there are remnants of amino groups and carboxylic groups that are not associated by coulumbic forces in the polyelectrolyte complexes. Free $-NH_2$ and −COOH active sites may form hydrogen bonding with −OH and $-COOCH_3$ from pectin. Theses interactions are sensible to dissociate at acidic and alkaline mediums, respectively (Yao et al., 1997). It was previously reported that in Ch-Pe composites, swell behavior is limited when 3< pH <8, however this values significantly increase when pH < 3 and pH> 8 due to the weak intermolecular forces through the dissociation of the hydrogen bonding (Tsai et al., 2014). These polymers were reported not to precipitate or solubilize until extreme conditions of pH and temperature (Sluiter et al., 2004), however, this phenomenon could explain the lower biosorption values in acidic (3-4) solutions in the present work (Fig. 4b). Thus, although there was a decrease in the adsorption capacity under the conditions analyzed, compared to the previously reported capacity for pristine algae (Flores-Chaparro et al., 2017), Ma–Ch–Pe composites have a great advantage over previous ones considering the strengthening of their physical properties, which allow them to be applied in a larger scale (e.g. pilot or industrial).

The influence of the surface charge in electrostatic interactions between adsorbate and adsorbent should be observed in organic ionizable compounds (i.e. dyes), but the molecules under study were in the non-ionizable form in the whole ranges of pH (Wibowo et al., 2007). In this case, hydrophobic interactions between the adsorbates and the lignin and lignocellulosic fraction of the macroalgae biomass would remain the main important fraction for biosorption.

3.3.3. Biosorption kinetics: Effect of dissolved organic matter (DOM)

To evaluate effects of DOM on the removal rate of benzene, toluene and naphthalene, experiments were carried out by using natural water from a reservoir containing 19.3 mg L^{-1} of DOM. The adsorption of HC in the presence of DOM (Fig. 5a,b) could be divided in two steps: external diffusion and surface adsorption. Both were promptly achieved through the former step, and the equilibrium was gradually reached in the second step. These results suggest that with the exception of *M. pyrifera* biomass, the biosorption capacity is mainly limited by external diffusion. The kinetic data were found to fit better the pseudo-second order kinetic equation (Table S10), with the exception of benzene, which has reported a slightly better approach to the pseudo-first order equation. HC rate removal increased (Fig. 5c) in natural water (NW) compared to deionized water (DW). In this sense, the biosorption capacity increased 33, 61 and 47 % for benzene, toluene and naphthalene, respectively.

Based in the literature the natural organic matter may promote a covalent bond with chitosan through carboxylic acid functional groups (Rangel-Mendez et al., 2009). The same kind of interaction could be expected from pectin, and the macroalgae biomass, because these fractions share the same surface active sites. Moreover, humic acids, which are present in DOM, have a significant degree of aromatic polymers, chemical compositions, functional groups (aliphatic and alicyclic) and charge density (Chon et al., 2017). The light absorbing fraction of DOM (CDOM) corroborated a high aromaticity degree ($SUVA_{254}$ = 0.976 L mg^{-1} m^{-1}), and the presence of higher molecular weight components like humic acids (E2: E3 ratio = 5.03). Humic acids are hypothesized

to have an open network forming aggregates with voids that could join to the Ma-Ch-Pe omposites, promoting hydrophobic and π interactions between the biosorbents and the aromatic hydrocarbons, explaining the increase on the removal capacity.

A comparison of the biosorption capacities of the HCs under study on different adsorbent surfaces and cellulosic precursors is presented in Table S11. The Ma−Ch−Pe composite in this study exhibited comparable biosorption capacities and even higher than other natural materials like wood chips or bagasse (Bandura et al., 2017; Flores-Chaparro et al., 2016, 2016; Hubbe et al., 2014; Mohamed and Ouki, 2011; Simantiraki et al., 2013; Yakout, 2014). Additionally, the biosorbent offers all the properties to be used in subsequent flow-through biosorption studies. Additionally, the biosorbent offers all the properties to be used in subsequent flow-through biosorption studies. Further research regarding to the dynamic biosorption of aromatic pollutants by the Ma-Ch-Pe biocomposite and the effect of multi-solute systems will be subject of future publications.

4. Conclusions

A factorial experiment design in conjunction with a surface response methodology were applied to find the optimal conditions (75.4%, 19.8, and 4.8% for macroalgae biomass, chitosan and pectin, respectively), to remove the highest benzene concentration from water, as an aromatic hydrocarbon model. The chitosan and algae biomass content were the main factors involved in the process. The biosorption mechanism is a sum of interactions between the diverse of chemical components of the composite precursors, and involves mainly hydrophobic effect between lipids and lignocellulosic fractions (cellulose, hemicellulose and lignin) and nonspecific van der Waals interactions with carbohydrates, proteins, chitosan and pectin contents. The pH of the system (3–9) has no significant effect in the removal capacity because of the non–ionizable character of the HCs. The hydrocarbons affinities were not affected at least up to I = 0.6 M, but at higher concentrations there was a decrease in the adsorption capacity by pore occlusion by water molecules and competition for surface active sites of the biocomposite. The presence of dissolved organic matter enhanced the biosorption capacity by the stimulation of hydrophobic interactions between the biosorbent and the adsorbates. Moreover, the results reported in the present work showed the potential of the synthesized composites to be applied in the removal of benzene, toluene and naphthalene from polluted natural water in batch processes. Future work to assess the feasibility of the biosorbents will include the set up of a continuous system, and incineration technologies of saturated materials. The experiments in the following study will also consider multicomponent systems, the bioavailability and toxicity to aquatic organisms.

Acknowledgements

This work was supported by grant PDCPN-01-247032. The authors acknowledges a doctoral and postdoctoral fellowship from CONACyT no. 424187 and 210643. The authors express their

gratitude to D.I. Partida, G. Vidriales, J.P. Rodas, E. Cortez and M.C. Rocha for their invaluable assistance throughout the investigation. The authors also thank CICIMAR-IPN and UABC research institutions for the macroalgae provided.

5. References

A. Pérez-Escobedo, P.E.D.-F., 2016. Fluoride adsorption capacity of composites based on chitosan zeolite-algae. Rev. Mex. Ing. Quím. 15, 139–147.

Angelova, R., Baldikova, E., Pospiskova, K., Maderova, Z., Safarikova, M., Safarik, I., 2016. Magnetically modified Sargassum horneri biomass as an adsorbent for organic dye removal. J. Clean. Prod. 137, 189–194. https://doi.org/10.1016/j.jclepro.2016.07.068

Antony, J., 2014. Design of Experiments for Engineers and Scientists. Elsevier.

Arafat, H.A., Franz, M., Pinto, N.G., 1999. Effect of Salt on the Mechanism of Adsorption of Aromatics on Activated Carbon†. Langmuir 15, 5997–6003. https://doi.org/10.1021/la9813331

Ata, A., Nalcaci, O.O., Ovez, B., 2012. Macro algae Gracilaria verrucosa as a biosorbent: A study of sorption mechanisms. Algal Res. 1, 194–204. https://doi.org/10.1016/j.algal.2012.07.001

Balaria, A., Schiewer, S., 2008. Assessment of biosorption mechanism for Pb binding by citrus pectin. Sep. Purif. Technol. 63, 577–581. https://doi.org/10.1016/j.seppur.2008.06.023

Bandosz, T.J., Jagiello, J., Contescu, C., Schwarz, J.A., 1993. Characterization of the surfaces of activated carbons in terms of their acidity constant distributions. Carbon 31, 1193–1202. https://doi.org/10.1016/0008-6223(93)90072-I

Bandura, L., Kołodyńska, D., Franus, W., 2017. Adsorption of BTX from aqueous solutions by Na-P1 zeolite obtained from fly ash. Process Saf. Environ. Prot. 109, 214–223. https://doi.org/10.1016/j.psep.2017.03.036

Benbouzid, H., Le Floch, S., Stephan, L., Olier, R., Privat, M., 2012. Combined effects of salinity and temperature on the solubility of organic compounds. J. Chem. Thermodyn. 48, 54–64. https://doi.org/10.1016/j.jct.2011.11.020

Brunauer, S., Emmett, P.H., Teller, E., 1938. Adsorption of Gases in Multimolecular Layers. J. Am. Chem. Soc. 60, 309–319. https://doi.org/10.1021/ja01269a023

Caetano, M.O., Schneider, I.A.H., Gomes, L.P., Kieling, A.G., Miranda, L.A.S., 2017. A compact remediation system for the treatment of groundwater contaminated with BTEX and TPH. Environ. Technol. 38, 1408–1420. https://doi.org/10.1080/09593330.2016.1231222

Chen, B., Wang, Y., Hu, D., 2010. Biosorption and biodegradation of polycyclic aromatic hydrocarbons in aqueous solutions by a consortium of white-rot fungi. J. Hazard. Mater. 179, 845–851. https://doi.org/10.1016/j.jhazmat.2010.03.082

Cho, J., Heuzey, M.-C., Bégin, A., Carreau, P.J., 2005. Physical Gelation of Chitosan in the Presence of β-Glycerophosphate: The Effect of Temperature. Biomacromolecules 6, 3267–3275. https://doi.org/10.1021/bm050313s

Chon, Kangmin, Chon, Kyongmi, Cho, J., 2017. Characterization of size fractionated dissolved organic matter from river water and wastewater effluent using preparative high performance size exclusion chromatography. Org. Geochem. 103, 105–112. https://doi.org/10.1016/j.orggeochem.2016.11.003

Chung, M.K., Tsui, M.T.K., Cheung, K.C., Tam, N.F.Y., Wong, M.H., 2007. Removal of aqueous phenanthrene by brown seaweed Sargassum hemiphyllum: Sorption-kinetic and equilibrium studies. Sep. Purif. Technol. 54, 355–362. https://doi.org/10.1016/j.seppur.2006.10.008

Crini, G., Badot, P.-M., 2008. Application of chitosan, a natural aminopolysaccharide, for dye removal from aqueous solutions by adsorption processes using batch studies: A review of

recent literature. Prog. Polym. Sci. 33, 399–447. https://doi.org/10.1016/j.progpolymsci.2007.11.001

Davila-Rodriguez, J.L., Escobar-Barrios, V.A., Shirai, K., Rangel-Mendez, J.R., 2009. Synthesis of a chitin-based biocomposite for water treatment: Optimization for fluoride removal. J. Fluor. Chem. 130, 718–726. https://doi.org/10.1016/j.jfluchem.2009.05.012

Eroglu, E., Smith, S.M., Raston, C.L., 2015. Application of Various Immobilization Techniques for Algal Bioprocesses, in: Moheimani, N.R., McHenry, M.P., Boer, K. de, Bahri, P.A. (Eds.), Biomass and Biofuels from Microalgae, Biofuel and Biorefinery Technologies. Springer International Publishing, pp. 19–44. https://doi.org/10.1007/978-3-319-16640-7_2

Flores-Chaparro, C.E., Chazaro Ruiz, L.F., Alfaro de la Torre, M.C., Huerta-Diaz, M.A., Rangel-Mendez, J.R., 2017. Biosorption removal of benzene and toluene by three dried macroalgae at different ionic strength and temperatures: Algae biochemical composition and kinetics. J. Environ. Manage. 193, 126–135. https://doi.org/10.1016/j.jenvman.2017.02.005

Flores-Chaparro, C.E., Ruiz, L.F.C., Torre, M.C.A.-D. la, Rangel-Mendez, J.R., 2016. Soluble hydrocarbons uptake by porous carbonaceous adsorbents at different water ionic strength and temperature: something to consider in oil spills. Environ. Sci. Pollut. Res. 1–11. https://doi.org/10.1007/s11356-016-6286-0

Hameed, M.S.A., 2006. Continuous removal and recovery of lead by alginate beads, free and alginate-immobilized Chlorella vulgaris. Afr. J. Biotechnol. 5. https://doi.org/10.4314/ajb.v5i19.55877

Hashemi, P., Bagheri, S., Fat'hi, M.R., 2005. Factorial design for optimization of experimental variables in preconcentration of copper by a chromotropic acid loaded Q-Sepharose adsorbent. Talanta 68, 72–78. https://doi.org/10.1016/j.talanta.2005.04.058

Heede, R., Oreskes, N., 2016. Potential emissions of CO2 and methane from proved reserves of fossil fuels: An alternative analysis. Glob. Environ. Change 36, 12–20. https://doi.org/10.1016/j.gloenvcha.2015.10.005

Hubbe, M.A., Park, J., Park, S., 2014. Cellulosic Substrates for Removal of Pollutants from Aqueous Systems: A Review. Part 4. Dissolved Petrochemical Compounds. BioResources 9, 7782–7925. https://doi.org/10.15376/biores.9.4.

Jagiello, J., 1994. Stable Numerical Solution of the Adsorption Integral Equation Using Splines. Langmuir 10, 2778–2785. https://doi.org/10.1021/la00020a045

Jeppu, G.P., Clement, T.P., 2012. A modified Langmuir-Freundlich isotherm model for simulating pH-dependent adsorption effects. J. Contam. Hydrol., Sorption and Transport Processes Affecting the Fate of Environmental Pollutants in the Subsurface 129–130, 46–53. https://doi.org/10.1016/j.jconhyd.2011.12.001

Jiang, Y., Gong, J.-L., Zeng, G.-M., Ou, X.-M., Chang, Y.-N., Deng, C.-H., Zhang, J., Liu, H.-Y., Huang, S.-Y., 2016. Magnetic chitosan–graphene oxide composite for anti-microbial and dye removal applications. Int. J. Biol. Macromol. 82, 702–710. https://doi.org/10.1016/j.ijbiomac.2015.11.021

Kyzas, G.Z., Bikiaris, D.N., 2015. Recent Modifications of Chitosan for Adsorption Applications: A Critical and Systematic Review. Mar. Drugs 13, 312–337. https://doi.org/10.3390/md13010312

Lamichhane, S., Bal Krishna, K.C., Sarukkalige, R., 2016. Polycyclic aromatic hydrocarbons (PAHs) removal by sorption: A review. Chemosphere 148, 336–353. https://doi.org/10.1016/j.chemosphere.2016.01.036

Lastoskie, C., Gubbins, K.E., Quirke, N., 1993. Pore size distribution analysis of microporous carbons: a density functional theory approach. J. Phys. Chem. 97, 4786–4796. https://doi.org/10.1021/j100120a035

Liu, Y., Kujawinski, E.B., 2015. Chemical Composition and Potential Environmental Impacts of Water-Soluble Polar Crude Oil Components Inferred from ESI FT-ICR MS. Plos One 10, e0136376. https://doi.org/10.1371/journal.pone.0136376

Liu, Y., Liu, Y.-J., 2008. Biosorption isotherms, kinetics and thermodynamics. Sep. Purif. Technol. 61, 229–242. https://doi.org/10.1016/j.seppur.2007.10.002

Marudova, M., MacDougall, A.J., Ring, S.G., 2004. Pectin–chitosan interactions and gel formation. Carbohydr. Res. 339, 1933–1939. https://doi.org/10.1016/j.carres.2004.05.017

Mohamed, M., Ouki, S., 2011. Removal Mechanisms of Toluene from Aqueous Solutions by Chitin and Chitosan. Ind. Eng. Chem. Res. 50, 9557–9563. https://doi.org/10.1021/ie200110t

Motlagh, S., Ravines, P., Ma, Q., Jaksch, F., 2000. Identification of Gum Arabic sing PAGE and IEF A2, in: Gums and Stabilisers for the Food Industry 10. Woodhead Publishing, pp. 53–58.

Myers, R.H., Montgomery, D.C., Anderson-Cook, C.M., 2016. Response Surface Methodology: Process and Product Optimization Using Designed Experiments. John Wiley & Sons.

Navarro, A.E., Lazo, J.C., Cuizano, N.A., Sun-Kou, M.R., Llanos, B.P., 2009. Insights into Removal of Phenol from Aqueous Solutions by Low Cost Adsorbents: Clays Versus Algae. Sep. Sci. Technol. 44, 2491–2509. https://doi.org/10.1080/01496390903012197

Njobuenwu, D.O., Amadi, S.A., Ukpaka, P.C., 2005. Dissolution Rate of BTEX Contaminants in Water. Can. J. Chem. Eng. 83, 985–989. https://doi.org/10.1002/cjce.5450830608

Pampanin, D.M., Sydnes, M.O., 2013. Polycyclic Aromatic Hydrocarbons a Constituent of Petroleum: Presence and Influence in the Aquatic Environment. https://doi.org/10.5772/48176

Pandey, S., Mishra, A., Raval, P., Patel, H., Gupta, A., Shah, D., 2013. Chitosan–pectin polyelectrolyte complex as a carrier for colon targeted drug delivery. J. Young Pharm. 5, 160–166. https://doi.org/10.1016/j.jyp.2013.11.002

Qiu, H., Lv, L., Pan, B., Zhang, Qing-jian, Zhang, W., Zhang, Quan-xing, 2009. Critical review in adsorption kinetic models. J. Zhejiang Univ. Sci. A 10, 716–724. https://doi.org/10.1631/jzus.A0820524

Rangel-Mendez, J.R., Monroy-Zepeda, R., Leyva-Ramos, E., Diaz-Flores, P.E., Shirai, K., 2009. Chitosan selectivity for removing cadmium (II), copper (II), and lead (II) from aqueous phase: pH and organic matter effect. J. Hazard. Mater. 162, 503–511. https://doi.org/10.1016/j.jhazmat.2008.05.073

Rathod, M., Mody, K., Basha, S., 2014. Efficient removal of phosphate from aqueous solutions by red seaweed, Kappaphycus alverezii. J. Clean. Prod., Special Volume: The sustainability agenda of the minerals and energy supply and demand network: an integrative analysis of ecological, ethical, economic, and technological dimensions 84, 484–493. https://doi.org/10.1016/j.jclepro.2014.03.064

Ravikumar, K., Deebika, B., Balu, K., 2005. Decolourization of aqueous dye solutions by a novel adsorbent: Application of statistical designs and surface plots for the optimization and regression analysis. J. Hazard. Mater. 122, 75–83. https://doi.org/10.1016/j.jhazmat.2005.03.008

Rinaudo, M., 2006. Chitin and chitosan: Properties and applications. Prog. Polym. Sci. 31, 603–632. https://doi.org/10.1016/j.progpolymsci.2006.06.001

Rubín, E., Rodríguez, P., Herrero, R., Sastre de Vicente, M.E., 2006. Biosorption of phenolic compounds by the brown alga Sargassum muticum. J. Chem. Technol. Biotechnol. 81, 1093–1099. https://doi.org/10.1002/jctb.1430

Santos, L., Pinto, A., Filipe, O., Cunha, Â., Santos, E.B.H., Almeida, A., 2016. Insights on the Optical Properties of Estuarine DOM – Hydrological and Biological Influences. PLOS ONE 11, e0154519. https://doi.org/10.1371/journal.pone.0154519

Schiewer, S., Wong, M.H., 2000. Ionic strength effects in biosorption of metals by marine algae. Chemosphere 41, 271–282. https://doi.org/10.1016/S0045-6535(99)00421-X

Schijf, J., Ebling, A.M., 2010. Investigation of the Ionic Strength Dependence of Ulva lactuca Acid Functional Group pKas by Manual Alkalimetric Titrations. Environ. Sci. Technol. 44, 1644–1649. https://doi.org/10.1021/es9029667

Shimizu, Y., Kono, K., Kim, I.S., Takagishi, T., 1995. Effects of added metal ions on the interaction of chitin and partially deacetylated chitin with an azo dye carrying hydroxyl groups. J. Appl. Polym. Sci. 55, 255–261. https://doi.org/10.1002/app.1995.070550208

Simantiraki, F., Kollias, C.G., Maratos, D., Hahladakis, J., Gidarakos, E., 2013. Qualitative determination and application of sewage sludge and municipal solid waste compost for BTEX removal from groundwater. J. Environ. Chem. Eng. 1, 9–17. https://doi.org/10.1016/j.jece.2013.02.002

Sluiter, A., Hames, B., Ruiz, R.O., Scarlata, C., Sluiter, J., Templeton, D., 2004. Determination of structural carbohydrates and lignin in biomass. ResearchGate 2011, 1–14.

Sriamornsak, P., 2011. Application of pectin in oral drug delivery. Expert Opin. Drug Deliv. 8, 1009–1023. https://doi.org/10.1517/17425247.2011.584867

Terinte, N., Ibbett, R., Schuster, K., 2011. Overview on native cellulose and microcrystalline cellulose I structure studied by X-ray diffraction (WAXD): Comparison between measurement techniques. Lenzing. Berichte 89.

Tsai, R.-Y., Chen, P.-W., Kuo, T.-Y., Lin, C.-M., Wang, D.-M., Hsien, T.-Y., Hsieh, H.-J., 2014. Chitosan/pectin/gum Arabic polyelectrolyte complex: Process-dependent appearance, microstructure analysis and its application. Carbohydr. Polym. 101, 752–759. https://doi.org/10.1016/j.carbpol.2013.10.008

Tsibranska, I., Hristova, E., 2011. Comparison of different kinetic models for adsorption of heavy metals onto activated carbon from apricot stones. Bulg. Chem. Commun. 43, 370–377.

Tsuzuki, S., 2005. Interactions with Aromatic Rings, in: Wales, D.J. (Ed.), Intermolecular Forces and Clusters I. Springer-Verlag, Berlin/Heidelberg, pp. 149–193.

US EPA, 2013. Basic Information about Benzene in Drinking Water [WWW Document]. URL http://water.epa.gov/drink/contaminants/basicinformation/benzene.cfm (accessed 1.21.14).

Vankar, P.S., Sarswat, R., Dwivedi, A.K., Sahu, R.S., 2013. An assessment and characterization for biosorption efficiency of natural dye waste. J. Clean. Prod., Special Volume: Water, Women, Waste, Wisdom and Wealth 60, 65–70. https://doi.org/10.1016/j.jclepro.2011.09.021

Volesky, B., 2007. Biosorption and me. Water Res. 41, 4017–4029. https://doi.org/10.1016/j.watres.2007.05.062

Wan Ngah, W.S., Teong, L.C., Hanafiah, M.A.K.M., 2011. Adsorption of dyes and heavy metal ions by chitosan composites: A review. Carbohydr. Polym. 83, 1446–1456. https://doi.org/10.1016/j.carbpol.2010.11.004

Wang, N., Zhang, Y., Zhu, F., Li, J., Liu, S., Na, P., 2014. Adsorption of soluble oil from water to graphene. Environ. Sci. Pollut. Res. 21, 6495–6505. https://doi.org/10.1007/s11356-014-2504-9

Wibowo, N., Setyadhi, L., Wibowo, D., Setiawan, J., Ismadji, S., 2007. Adsorption of benzene and toluene from aqueous solutions onto activated carbon and its acid and heat treated forms: Influence of surface chemistry on adsorption. J. Hazard. Mater. 146, 237–242. https://doi.org/10.1016/j.jhazmat.2006.12.011

Xie, W.-H., Shiu, W.-Y., Mackay, D., 1997. A review of the effect of salts on the solubility of organic compounds in seawater. Mar. Environ. Res. 44, 429–444. https://doi.org/10.1016/S0141-1136(97)00017-2

Yakout, S.M., 2014. Removal of the hazardous, volatile, and organic compound benzene from aqueous solution using phosphoric acid activated carbon from rice husk. Chem. Cent. J. 8, 52. https://doi.org/10.1186/s13065-014-0052-5

Yang, F., Liu, H., Qu, J., Paul Chen, J., 2011. Preparation and characterization of chitosan encapsulated Sargassum sp. biosorbent for nickel ions sorption. Bioresour. Technol. 102, 2821–2828. https://doi.org/10.1016/j.biortech.2010.10.038

Yang, X., Tu, Y., Li, L., Shang, S., Tao, X., 2010. Well-Dispersed Chitosan/Graphene Oxide Nanocomposites. ACS Appl. Mater. Interfaces 2, 1707–1713. https://doi.org/10.1021/am100222m

Yao, K.D., Tu, H., Cheng, F., Zhang, J.W., Liu, J., 1997. pH-sensitivity of the swelling of a chitosan-pectin polyelectrolyte complex. Angew. Makromol. Chem. 245, 63–72. https://doi.org/10.1002/apmc.1997.052450106

Zhang, D., Ran, C., Yang, Y., Ran, Y., 2013. Biosorption of phenanthrene by pure algae and field-collected planktons and their fractions. Chemosphere 93, 61–68. https://doi.org/10.1016/j.chemosphere.2013.04.068

Zhao, H., Yan, H., Dong, S., Zhang, Y., Sun, B., Zhang, C., Ai, Y., Chen, B., Liu, Q., Sui, T., Qin, S., 2011. Thermogravimetry study of the pyrolytic characteristics and kinetics of macro-algae Macrocystis pyrifera residue. J. Therm. Anal. Calorim. 111, 1685–1690. https://doi.org/10.1007/s10973-011-2102-8

Ziolli, R.L., Jardim, W.F., 2002. Photocatalytic decomposition of seawater-soluble crude-oil fractions using high surface area colloid nanoparticles of TiO2. J. Photochem. Photobiol. Chem. 147, 205–212. https://doi.org/10.1016/S1010-6030(01)00600-1

Table 1. FTIR characteristic bands of Ma, Ch, Pe and Ma−Ch−Pe biocomposites.

Ma (cm^{-1})	Ch (cm^{-1})	Pe (cm^{-1})	Ma-Ch-Pe (cm^{-1})	Vibration assignment
3338	3352	3354	3309	H−O; N−H
2915	2916	2918	2940	C−H (sp^3); N-H
2848	2863	-	2863	-CH_2; N-H
-	1748	1730	1764	C=O (-COOH)
1638	1654	-	-	N-H; C=O
-	1590	1600	1597	C=C; C=O
1407	1424	-	1420	-CHO; CH_3·SO_2
-	1381	-	-	-CH; -SO_2; -CO_2
1338	1313	1222	1316	-CO; SO_2; -CO; -OH
1155	1147	-	-	-CO; C-O-C
1074	1068	1094	-	C-O-C; C-N
1020	1032	1012	1025	C-O
822	892	830	895	C-O-C; S-O; C-N; C-H
592	676	-	680	C−O

Table 2. Parameters of the isotherm equations, correlation coefficients (R^2) and error function values of the models for organic compounds adsorption.

	Ma–Ch–Pe composite		
	Benzene	Toluene	Naphthalene
Langmuir			
q_{max} (mg·g^{-1})	67.71	20.45	8.80
b (L·mg^{-1})	0.002	0.008	0.255
R_L	0.207	0.186	0.121
SSE	72.10	11.57	2.57
R^2	0.979	0.964	0.973
Freundlich			
n	0.446	0.421	0.516
K_F	2.08	1.25	2.01
SSE	208.11	28.92	5.52
R^2	0.942	0.911	0.887
Sips			
b	0.0004	0.0007	0.227
q_{max} (mg·g^{-1})	58.08	16.64	6.13
n (L·mg^{-1})	1.35	1.61	2.096
R_L	0.587	0.719	0.134
SSE	42.47	4.69	0.35
R^2	0.988	0.985	0.992

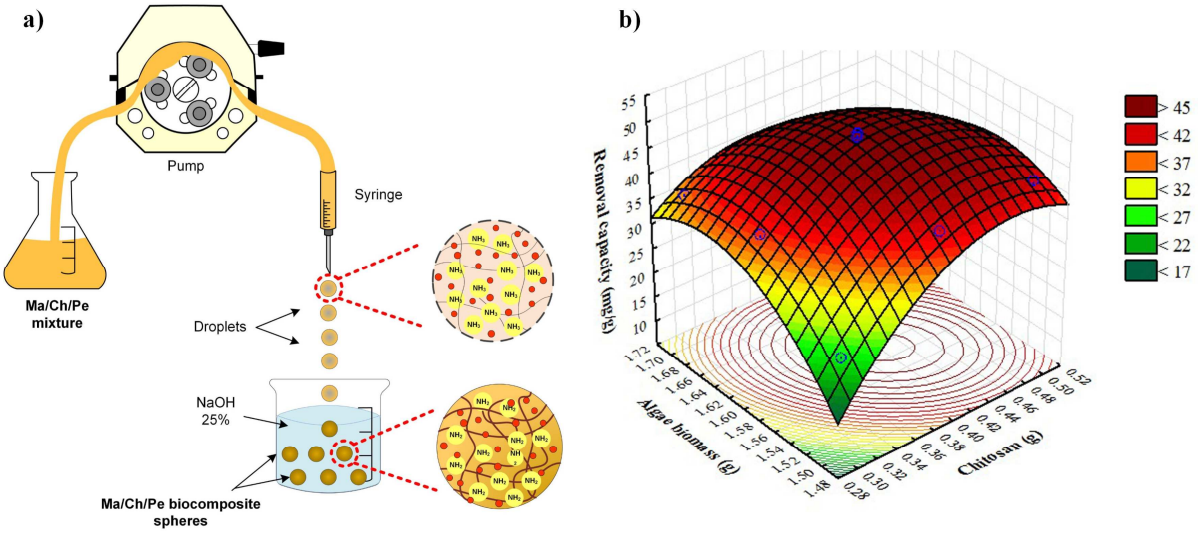

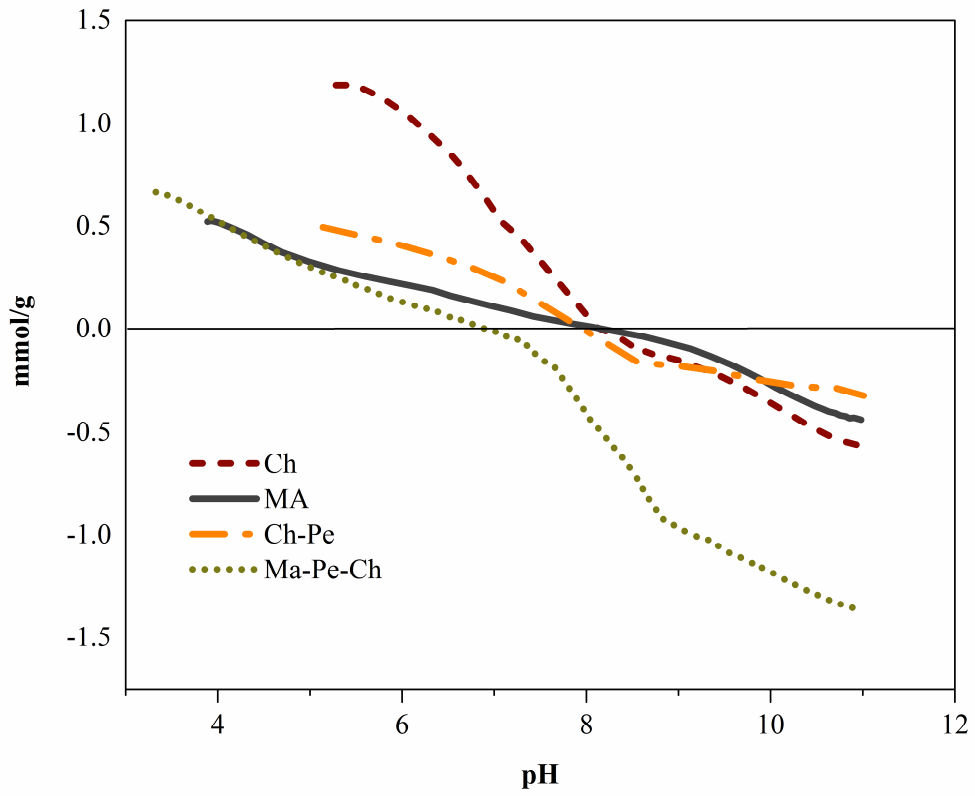

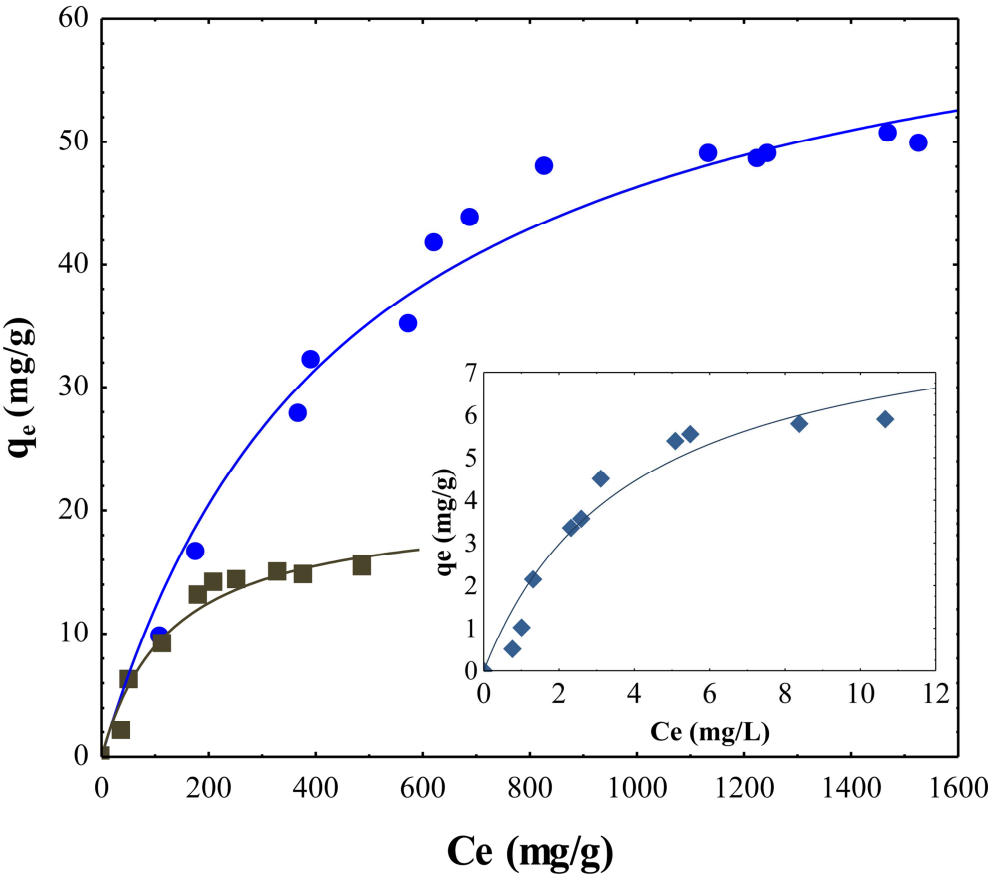
60
50
40
30
20
10
0
q_e (mg/g)
0
200
400
600
800
1000
1200
1400
1600
Ce (mg/g)
7
6
5
4
3
2
1
0
qe (mg/g)
0
2
4
6
8
10
12
Ce (mg/L)

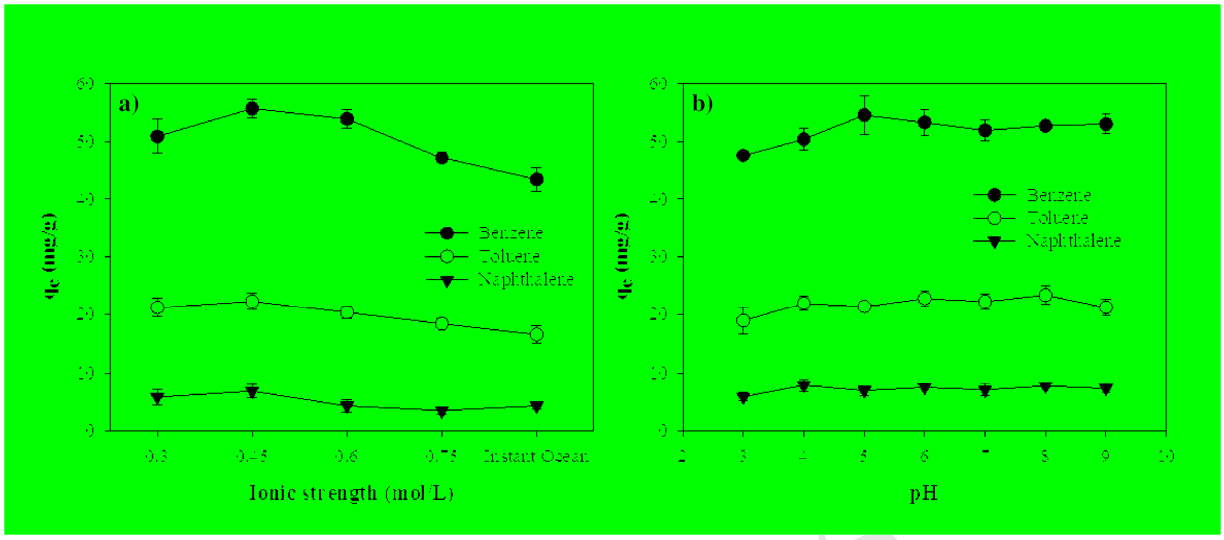

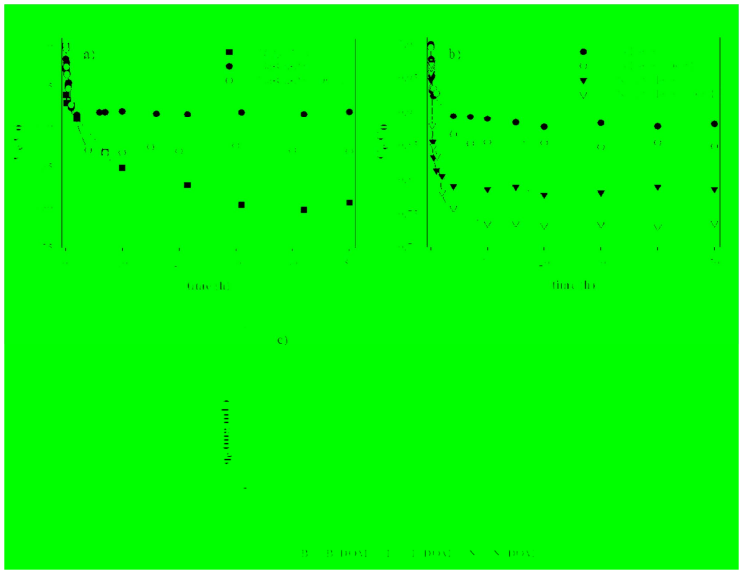

Figure captions

Fig. 1. (a) Drop system for biocomposite synthesis; (b) Response surface contour plot of benzene removal (mg g–1) showing interactive effect of macroalgae biomass (g) and chitosan (g).

Fig. 2. (b) Surface charge Ma−Ch−Pe, Ch-Pe and the precursors Ma, Ch and Pe as a function of pH.

Fig. 3. Adsorption isotherm of (●) benzene, (■) toluene and (◆) naphthalene at initial pH 6 − 7, and 25°C. The lines represent the Sips adsorption isotherm equation.

Fig. 4. (a) Effect of the ionic strength on the biosorption capacities of benzene, toluene and naphthalene by Ma–Ch–Pe biocomposite; (b) pH effect of benzene, toluene and naphthalene uptake by Ma–Ch–Pe biocomposite.

Fig. 5. (a) Benzene biosorption rate onto (■) macroalgae biomass, (●) Ma−Ch−Pe, (○) Ma−Ch−Pe and dissolved organic matter (DOM); (b) Effect of DOM in the rate of adsorption of (●) toluene, (○) toluene + DOM, (▼) naphthalene, (▽) naphthalene + DOM; (c) Adsorption capacity of benzene, toluene and naphthalene in the presence of organic matter.

Highlights

- Chitosan, pectin and macroalgae were used to synthesize a new biocomposite
- A surface response methodology was applied to maximize the adsorption capacity
- The adsorption capacity was slightly influenced by the pH and by the ionic strength
- The presence of DOM enhanced the removal of soluble hydrocarbons
- Synthesized composites are an excellent option to be applied in continuous systems